Supplementary Materials for Continual Learning with Node-Importance based Adaptive Group Sparse Regularization

Sangwon Jung[1]*, Hongjoon Ahn[2]*, Sungmin Cha[1] and Taesup Moon[1,2]
[1]Department of Electrical and Computer Engineering, [2] Department of Artificial Intelligence,
Sungkyunkwan University, Suwon, Korea 16419
{s.jung, hong0805, csm9493, tsmoon}@skku.edu

1 Proof of Lemma 1

From (Eq.(3), manuscript), $\mathbf{prox}_{\alpha f}(\boldsymbol{v})$ minimizes the convex function

$$\ell(\boldsymbol{\theta}) \triangleq c\|\boldsymbol{\theta}-\boldsymbol{\theta}_0\|_2 + \frac{1}{2\alpha}\|\boldsymbol{\theta}-\boldsymbol{v}\|_2^2, \tag{1}$$

and for brevity, denote $\boldsymbol{\theta}^* := \mathbf{prox}_{\alpha f}(\boldsymbol{v})$ as the minimizer. Denoting $\partial_{\boldsymbol{\theta}}\ell(\boldsymbol{\theta})$ as the set of subgradients of $\ell(\boldsymbol{\theta})$, we know that $\boldsymbol{\theta}^* \in \{\boldsymbol{\theta} : \partial_{\boldsymbol{\theta}}\ell(\boldsymbol{\theta}) = 0\}$ since $\ell(\boldsymbol{\theta})$ is convex. Also, by denoting $\boldsymbol{w}$ as the subgradient of $\|\boldsymbol{\theta}-\boldsymbol{\theta}_0\|_2$ at $\boldsymbol{\theta}^*$, we then have the optimality condition,

$$\frac{1}{\alpha}(\boldsymbol{v}-\boldsymbol{\theta}^*) = c\boldsymbol{w}. \tag{2}$$

Since $\|\boldsymbol{\theta}-\boldsymbol{\theta}_0\|_2$ is not differentiable at $\boldsymbol{\theta}=\boldsymbol{\theta}_0$, we know

$$\boldsymbol{w} = \begin{cases} \frac{\boldsymbol{\theta}^*-\boldsymbol{\theta}_0}{\|\boldsymbol{\theta}^*-\boldsymbol{\theta}_0\|_2} & \text{if } \boldsymbol{\theta}^* \neq \boldsymbol{\theta}_0 \\ \in \{\boldsymbol{w} : \|\boldsymbol{w}\|_2 < 1\} & \text{if } \boldsymbol{\theta}^* = \boldsymbol{\theta}_0 \end{cases}. \tag{3}$$

Now, taking ℓ_2-norm on both sides of (2), we can deduce

$$\boldsymbol{\theta}^* = \boldsymbol{\theta}_0 \text{ if and only if } \|\boldsymbol{v}-\boldsymbol{\theta}^*\|_2 < \alpha c. \tag{4}$$

Moreover, if $\boldsymbol{\theta}^* \neq \boldsymbol{\theta}_0$, we can derive from (2) and (3) that

$$\|\boldsymbol{v}-\boldsymbol{\theta}_0\|_2 - \alpha c = \|\boldsymbol{\theta}^*-\boldsymbol{\theta}\|_2 \geq 0, \tag{5}$$

and correspondingly,

$$\boldsymbol{\theta}^* = \Big(1-\frac{\alpha c}{\|\boldsymbol{\theta}_0-\boldsymbol{v}\|_2}\Big)\boldsymbol{v} + \frac{\alpha c}{\|\boldsymbol{\theta}_0-\boldsymbol{v}\|_2}\boldsymbol{\theta}_0. \tag{6}$$

Combining (4) and (6), we have the lemma. ■

2 Additional ablation studies

2.1 Ablation study of ρ

Here, we analyze the effect of ρ for the **[Rand-init]** described in Section 3.4 (manuscript) (I.2). Figure 1 below reports the average accuracy on CIFAR-100 for AGS-CL and MAS. For AGS-CL, we fixed $(\mu,\lambda)=(10,400)$ and varied $\rho\in\{0.1,\dots,0.5\}$, and for MAS, we used the optimal hyperparameter.

*Equal contribution.

34th Conference on Neural Information Processing Systems (NeurIPS 2020), Vancouver, Canada.

First, we observe that for $\rho \leq 0.5$, AGS-CL is not very sensitive to ρ, and it outperforms MAS for all ρ. Second, we observe that ρ affects the plasticity for learning new tasks. Namely, while $\rho = 0.1$ and $\rho = 0.5$ achieve the same final average accuracy, we note $\rho = 0.1$ suffers earlier since it does not sufficiently grow the network capacity for learning new tasks, whereas $\rho = 0.5$ suffers later since it uses up the network capacity too much in early tasks and makes the network too stable for later tasks. Thus, appropriate ρ may find the right trade-off between the sparsity and the used capacity of the network and achieve higher average accuracy.

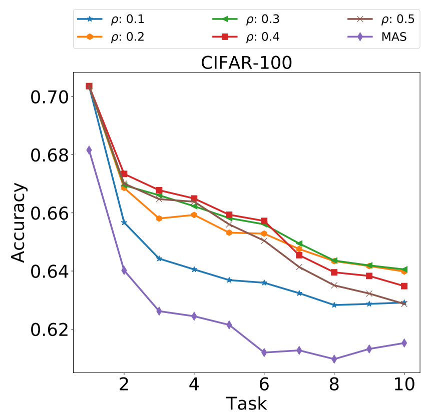

Figure 1: Average accuracy of AGS-CL on CIFAR-100 depending on ρ

2.2 Effect of PGD updates

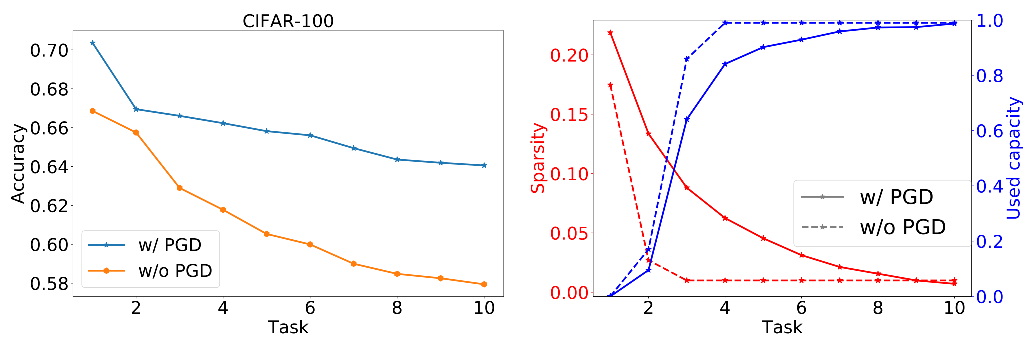

(a) Average accuracy with and without PGD.

(b) Sparsity (decreasing curves) and used capacity (increasing curves) with and without PGD.

Figure 2: Ablation study on PGD for CIFAR-100

As mentioned in Section 3.3 (manuscript), our PGD update plays a critical role in achieving high accuracy. Here, we compare with a method without PGD. Figure 2(a) and Figure 2(b) show the average accuracy and the sparsity and used capacity on CIFAR-100. '*w/o* PGD' in Figure 2 indicates training the network without PGD, *i.e.*, the Adam step was used for optimizing $\mathcal{L}_t(\boldsymbol{\theta})$ (Eq.(2), manuscript) which implies the combined loss of $\mathcal{L}_{\text{TS},t}(\boldsymbol{\theta})$ and group sparse regularizations(term (a) and term (b) of Eq.(2), manuscript). Since optimizing $\mathcal{L}_t(\boldsymbol{\theta})$ using Adam cannot achieve the global optimal point of group sparse regularization, we used a proper threshold τ to modify the definition of $\mathcal{G}_0$ in (Eq.(1), manuscript) and the used capacity. Thus, we define $\mathcal{G}_0^{t-1} \triangleq \{n_\ell : \Omega_{n_\ell}^{t-1} < \tau\} \subseteq \mathcal{G}$, and used capacity as $|\{n_\ell : \|\hat{\boldsymbol{\theta}}_{n_\ell}^{(t)} - \hat{\boldsymbol{\theta}}_{n_\ell}^{(t-1)}\|_2 < \tau\}|/|\mathcal{G}|$. Except for above definitions, all the common hyperparameters and training settings are same as '*w/* PGD', and we set the threshold $\tau = 10^{-4}$.

Followings are our observations. First, the average accuracy (Figure 2(a)) of '*w/o* PGD' is much lower than '*w/* PGD', which indicates that our PGD updates not only require *less* hyperparameters (*i.e.*, does not need τ threshold), but also does a much more accurate sparsification and freezing for achieving high accuracy. Second, we observe the sparsity (Figure 2(b)) of '*w/o* PGD' decreases much faster than '*w/* PGD'. The reason is because the weights associated with the nodes in $\mathcal{G}_0^t$ are not exactly zero, hence, the gradients for those weights do not vanish, which cause the unimportant nodes in $\mathcal{G}_0^t$ also continuously learn in every task. From these results, we conclude our PGD update is essential in AGS-CL.

2.3 Comparison with EWC

We additionally evaluate the performance of EWC with two measures, plasticity ($\mathcal{P}$) and stability ($\mathcal{S}$), which are proposed in (Figure 5(c), manuscript). Figure 3 reports the trade-offs between $\mathcal{P}$ and $\mathcal{S}$ for AGS-CL, MAS and EWC. The plotted trade-offs of EWC are over the λ and the others are the same as (Figure 5(c), manuscript). Note that although EWC has comparable $\mathcal{P}$-$\mathcal{S}$ trade-offs with MAS, AGS-CL apparently has the better $\mathcal{P}$-$\mathcal{S}$ trade-offs than EWC and MAS.

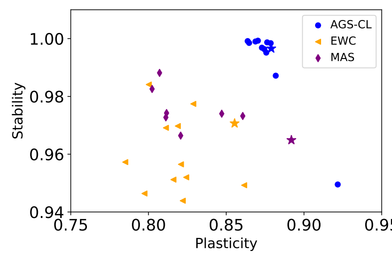

Figure 3: Plasticity ($\mathcal{P}$) and stability ($\mathcal{S}$) for CIFAR-100

3 Implementation details

3.1 Supervised learning

In CIFAR-100, CIFAR-10/100 and Omniglot [2], we train all methods with mini-batch size of 256 for 100 epochs using Adam optimizer [1] with initial learning rate 0.001 and decaying it by a factor of 3 if there is no improvement in the validation loss for 5 consecutive epochs, similarly as in [4]. In CUB200[3], we train all methods with mini-batch size 64 for 40 epochs using SGD with momentum 0.9 with initial learning rate 0.005 and decay it by a factor of 10 after training 30 epochs.

3.1.1 Hyperparameters for supervised learning experiments

The details on hyperparameters are in Table 1. For AGS-CL, we set η to 0.9 and for RWALK, we set α to 0.9 for all datasets. We extensively searched the best hyperparameter for each method to make the comparison as fair as possible.

Table 1: Hyperparameters for supervised learning experiments

Methods\Dataset	CIFAR-100	CIFAR-10/100	Omniglot	CUB200	Sequence of 8 different datasets
AGS-CL	λ (400) μ(10), ρ(0.3)	λ (7000) μ(20), ρ(0.2)	λ (1000) μ(7), ρ(0.5)	λ (1.5) μ(0.5), ρ(0.1)	λ (400000) μ(40), ρ(0.4)
EWC	λ (10000)	λ (25000)	λ (500000)	λ (40)	λ (1000)
SI	c (1.0)	c (0.7)	c (0.85)	c (0.75)	-
RWALK	λ (8)	λ (6)	λ (70)	λ (50)	-
MAS	λ (4)	λ (1)	λ (7)	λ (0.6)	λ (0.1)
HAT	c (2.5), smax(400)	c (0.1), smax(400)	c (2.5), smax(400)	-	-

3.1.2 Details on network architectures

The details on network architectures for CIFAR-100, CIFAR-10/100 and Omniglot are in Table 2 and 3. Since the number of classes for each task is different in Omniglot, we denoted the classes of ith task as C_i. For CUB200, we use the AlexNet architecture from PyTorch official models. [4]. For the sequence of 8 different datasets, we use the model of which the size of kernel is changed to 3×3 and the rest is the same as AlexNet.

Table 2: Network architecture for CIFAR-100 and CIFAR-10/100

Layer	Channel	Kernel	Stride	Padding	Dropout
32×32 input	3				
Conv 1	32	3×3	1	1	
Conv 2	32	3×3	1	1	
MaxPool			2	0	0.25
Conv 3	64	3×3	1	1	
Conv 4	64	3×3	1	1	
MaxPool			2	0	0.25
Conv 5	128	3×3	1	1	
Conv 6	128	3×3	1	1	
MaxPool			2	1	0.25
Dense 1	256				
Task 1 : Dense 10					
...					
Task i : Dense 10					

Table 3: Network architecture for Omniglot

Layer	Channel	Kernel	Stride	Padding	Dropout
28×28 input	1				
Conv 1	64	3×3	1	0	
Conv 2	64	3×3	1	0	
MaxPool			2	0	0
Conv 3	64	3×3	1	0	
Conv 4	64	3×3	1	0	
MaxPool			2	0	0
Task 1 : Dense C_1					
...					
Task i : Dense C_i					

3.1.3 Result tables

Table 4 shows the detailed results used to generate (Figure 4, manuscript). The number in the paranthesis with $\pm$ sign stands for the standard deviation of the accuracy obtained from 5 independent runs with different random seeds.

3.2 Reinforcement learning

3.2.1 Details on network architectures

For training Atari 8 tasks, we used the same architecture which was proposed in [2]. However, to secure the model capacity for training 8 tasks well enough, we implemented each layer that has four times more filters than the original architecture. Figure 5 shows the details of our model.

3.2.2 Hyperparameters of PPO

We used PPO [3] as an algorithm for training Atari 8 tasks. Figure 6 shows hyperparameters that we used for 8 tasks, and these hyperparameters are equally applied to each baseline. We evaluate each method every 40 updates, *i.e.* we have 30 evaluation results during training each task. We trained the model using Adam optimizer with the initial learning rate of 0.0003 and the other hyperparameters are same as [3].

[2] https://drive.google.com/file/d/1WxFZQyt3v7QRHwxFbdb1KO02XWLT0R9z/view?usp=sharing
[3] https://github.com/visipedia/tf_classification/wiki/CUB-200-Image-Classification
[4] https://github.com/pytorch/vision/blob/master/torchvision/models/alexnet.py

Table 4: Average accuracy(%) and standard deviation for 5 random seeds

	AGS-CL	EWC	SI	RWLAK	MAS	HAT
CIFAR-100	**64.1** ($\pm$1.7)	60.2 ($\pm$1.1)	60.3 ($\pm$1.3)	58.1 ($\pm$1.7)	61.5 ($\pm$0.9)	59.2 ($\pm$0.7)
CIFAR-10/100	**76.1** ($\pm$0.4)	70.0 ($\pm$0.3)	71.5 ($\pm$0.5)	69.6 ($\pm$1.1)	72.1 ($\pm$0.7)	59.8 ($\pm$1.6)
Omniglot	**82.8** ($\pm$1.8)	76.0 ($\pm$20.2)	54.9 ($\pm$16.2)	71.0 ($\pm$5.6)	81.4 ($\pm$2.1)	5.5 ($\pm$11.1)
CUB200	**81.9** ($\pm$0.7)	80.5 ($\pm$1.2)	80.4 ($\pm$0.8)	81.0 ($\pm$1.3)	79.6 ($\pm$1.0)	-
Sequence of 8 different datasets	**57.7** ($\pm$0.7)	52.2 ($\pm$2.9)	-	-	41.5 ($\pm$4.2)	-

Table 5: Network architecture for Atari

Layer	Channel	Kernel	Stride	Padding	Dropout
84$\times$84 input	4				
Conv 1	32$\times$4	8$\times$8	4	0	
ReLU					
Conv 2	32$\times$4	4$\times$4	2	0	
ReLU					
Conv 2	64$\times$4	3$\times$3	1	0	
ReLU					
Flatten					
Linear1	32$\times$4$\times$7$\times$7				
Task 1 : Dense C_1					
$\cdots$					
Task i : Dense C_i					

3.2.3 Detailed experimental results with $\mu = 0.1$

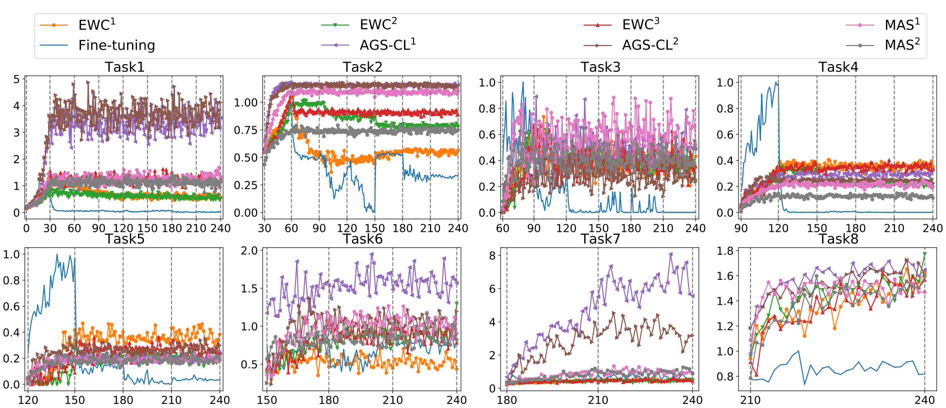

Figure 4: Reinforcement learning results. $\lambda = \{1, 2.5, 10\} \times 10^4$ for EWC^{1,2,3}, $\lambda = \{1, 10\}$ for MAS^{1,2}, and $\mu = 0.1$, $\lambda = \{1, 10\} \times 10^2$ for AGS-CL^{1,2} were used, respectively.

Figure 4 shows detailed rewards during training each task. From this figure, we can clearly observe that AGS-CL outperforms EWC for Task 1, 2 and 7 significantly. Especially, for Task 7, AGS-CL showed higher rewards than Fine-tuning, which means it achieves significantly higher plasticity. We also note that AGS-CL has higher stability than other baselines for all λ.

3.2.4 Additional experimental results with $\mu = 0.125$

To show the other result with a different μ, we selected $\mu = 0.125$ and experimented in Atari 8 tasks. From Figure 5, we observed that AGS-CL also achieves the highest reward , which is proposed in the manuscript, using $\mu = 0.1$ if we set an appropriate λ for AGS-CL. Figure 6 shows detailed experimental results with $\mu = 0.125$. There is a little difference with the reward of each task in Figure 4 but we observed that AGS-CL shows similar advantages which we already mentioned in Section 3.2.3.

Table 6: Details on hyperparameters of PPO.

Hyperparameters	Value
# of steps of each task	10^7
# of processes	128
# of steps per iteration	64
PPO epochs	10
entropy coefficient	0
value loss coefficient	0.5
γ for accumulated rewards	0.99
λ for GAE	0.95
mini-batch size	64

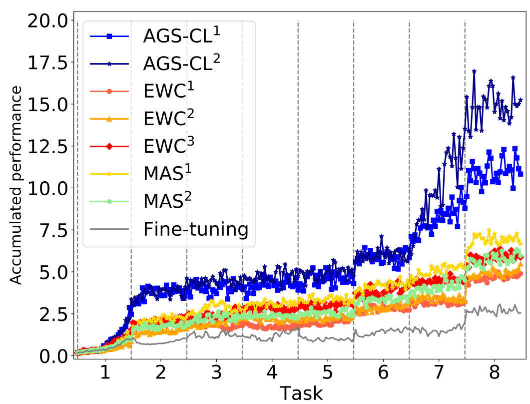

Figure 5: Normalized accumulated rewards. $\lambda = \{1, 2.5, 10\} \times 10^4$ for EWC^{1,2,3}, $\lambda = \{1, 10\}$ for MAS^{1,2}, and $\mu = 0.125$, $\lambda = \{1, 10\} \times 10^2$ for AGS-CL^{1,2} were used, respectively.

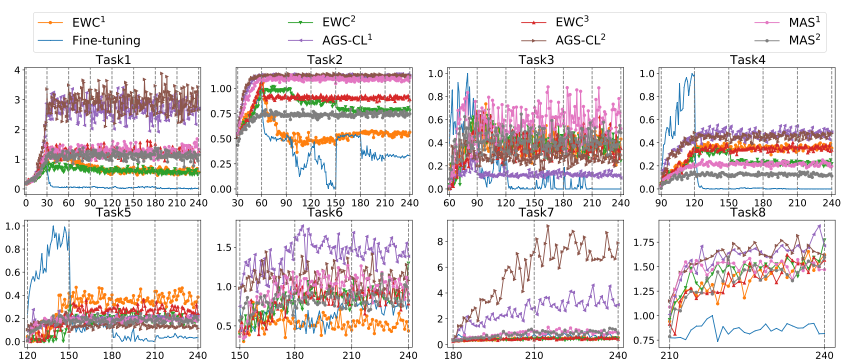

Figure 6: Reinforcement learning results. $\lambda = \{1, 2.5, 10\} \times 10^4$ for EWC^{1,2,3}, $\lambda = \{1, 10\}$ for MAS^{1,2}, and $\mu = 0.125$, $\lambda = \{1, 10\} \times 10^2$ for AGS-CL^{1,2} were used, respectively.

References

[1] Diederick P Kingma and Jimmy Ba. Adam: A method for stochastic optimization. In *International Conference on Learning Representations (ICLR)*, 2015.

[2] Volodymyr Mnih, Koray Kavukcuoglu, David Silver, Alex Graves, Ioannis Antonoglou, Daan Wierstra, and Martin Riedmiller. Playing atari with deep reinforcement learning. *arXiv preprint arXiv:1312.5602*, 2013.

[3] John Schulman, Filip Wolski, Prafulla Dhariwal, Alec Radford, and Oleg Klimov. Proximal policy optimization algorithms. *arXiv preprint arXiv:1707.06347*, 2017.

[4] Joan Serra, Didac Suris, Marius Miron, and Alexandros Karatzoglou. Overcoming catastrophic forgetting with hard attention to the task. In *International Conference on Machine Learning*

(ICML), pages 4548–4557, 2018.